

DISCOVERY OF A KILOPARSEC SCALE X-RAY/RADIO JET IN THE $Z = 4.72$ QUASAR GB 1428+4217

C. C. CHEUNG¹, L. STAWARZ^{2,3}, A. SIEMIGINOWSKA⁴, D. GOBEILLE^{5,6}, J. F. C. WARDLE⁵, D. E. HARRIS⁴,
D. A. SCHWARTZ⁴

ApJL, accepted

ABSTRACT

We report the discovery of a one-sided $3.6''$ (24 kpc, projected) long jet in the high-redshift, $z=4.72$, quasar GB 1428+4217 in new *Chandra* X-ray and VLA radio observations. This is the highest redshift kiloparsec-scale X-ray/radio jet known. Analysis of archival VLBI 2.3 and 8.6 GHz data reveal a faint one-sided jet extending out to ~ 200 parsecs and aligned to within $\sim 30^\circ$ of the *Chandra*/VLA emission. The $3.6''$ distant knot is not detected in an archival *HST* image, and its broad-band spectral energy distribution is consistent with an origin from inverse Compton scattering of cosmic microwave background photons for the X-rays. Assuming also equipartition between the radiating particles and magnetic field, the implied jet Lorentz factor is ≈ 5 . This is similar to the other two known $z \sim 4$ kpc-scale X-ray jet cases and smaller than typically inferred in lower-redshift cases. Although there are still but a few such very high-redshift quasar X-ray jets known, for an inverse Compton origin, the present data suggest that they are less relativistic on large-scales than their lower-redshift counterparts.

Subject headings: Galaxies: active — galaxies: jets — quasars: individual (GB 1428+4217) — radiation mechanisms: non-thermal — radio continuum: galaxies — X-rays: galaxies

1. INTRODUCTION

The $z = 4.72$ quasar GB 1428+4217 (B3 1428+422) was identified in a search for high-redshift objects through targeted optical spectroscopy of flat-spectrum radio sources (Hook & McMahon 1998; Fabian et al. 1997). It is a luminous X-ray source with detected X-ray and radio variability characteristic of a blazar (Fabian et al. 1999; Worsley et al. 2006; Veres et al. 2010). On parsec-scale, VLBA 15 GHz images indicate a dominant high brightness temperature, $T_b \simeq (4 - 6) \times 10^{11}$ K, core component with a faint one-sided jet-like extension (Veres et al. 2010, and references therein). The high luminosity, variability, and radio compactness are all properties consistent with Doppler beaming of emission from a relativistic jet aligned close to our line of sight (see Fabian et al. 1999).

Such high-redshift radio/X-ray sources offer a unique glimpse into powerful outbursts from active galactic nuclei (AGN) in the early Universe. As the ambient medium into which large-scale jets propagate (including host galaxy environments and intergalactic medium) is expected to be drastically different at such early epochs (e.g., De Young 2006; Miley & De Breuck 2008), studies of large-scale jet structures allow us to probe radio source interactions with their environment. Motivated by X-

ray detections of kpc-scale jets in two very high-redshift quasars, 1745+624 at $z = 3.9$ (Cheung et al. 2006) and GB 1508+5714 at $z = 4.3$ (Siemiginowska et al. 2003; Yuan et al. 2003), and the noticeable dearth of *Chandra* observations of $z \gtrsim 2$ jet systems (e.g., Kataoka & Stawarz 2005; Harris & Krawczynski 2006; Massaro et al. 2011), we began a program to obtain arcsecond-resolution radio and X-ray imaging of more such systems (Cheung et al. 2005, 2008) with the aim to understand the physics of the highest-redshift relativistic jets.

Using *Chandra* X-ray Observatory and NRAO⁷ Very Large Array (VLA) imaging observations of GB 1428+4217, we discovered an X-ray/radio jet separated from the nucleus by $3.6''$ (24 kpc, projected)⁸. At $z = 4.72$, this is the most distant kpc-scale jet imaged in X-rays. No significant optical emission is detected from the $3.6''$ knot in an archival *Hubble Space Telescope* (*HST*) image. To probe smaller scale emission, we imaged archival very long baseline interferometry (VLBI) 2.3 and 8.6 GHz data, revealing a one-sided ~ 200 parsec long jet aligned within $\sim 30^\circ$ of the kpc-scale *Chandra*/VLA structure. In the following, we present these multi-wavelength observations (Section 2), and go on to discuss the physical parameters of the large-scale outflow in terms of inverse Compton emission models, comparing this case to other X-ray detected AGN jets (Section 3).

2. RADIO, X-RAY, AND OPTICAL OBSERVATIONS

As part of a larger survey search for kpc-scale jets in a sample of $z \gtrsim 3.4$ flat-spectrum radio sources (Cheung et al. 2005), we obtained VLA A-array observa-

¹ National Research Council Research Associate, National Academy of Sciences, Washington, DC 20001, resident at Naval Research Laboratory, Washington, DC 20375, USA; Teddy.Cheung.ctr@nrl.navy.mil

² Institute of Space and Astronautical Science, Japan Aerospace Exploration Agency, 3-1-1 Yoshinodai, Chuo-ku, Sagami-hara, Kanagawa 252-5210, Japan

³ Astronomical Observatory, Jagiellonian University, ul. Orla 171, 30-244, Kraków, Poland

⁴ Harvard-Smithsonian Center for Astrophysics, 60 Garden St., Cambridge, MA 02138, USA

⁵ Department of Physics, MS 057, Brandeis University, Waltham, MA 02454, USA

⁶ Department of Physics, University of South Florida, Tampa, FL 33620, USA

⁷ The National Radio Astronomy Observatory is operated by Associated Universities, Inc. under a cooperative agreement with the National Science Foundation.

⁸ Adopting $H_0 = 71 \text{ km s}^{-1} \text{ Mpc}^{-1}$, $\Omega_M = 0.27$ and $\Omega_\Lambda = 0.73$, the quasar is at a luminosity distance, $D_L = 44.5 \text{ Gpc}$ and $1'' = 6.59 \text{ kpc}$.

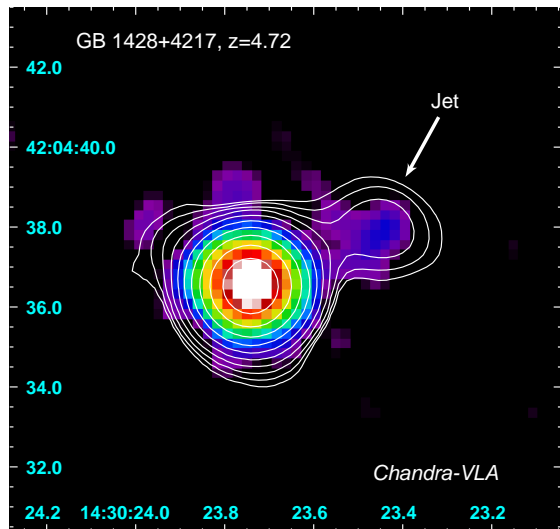


FIG. 1.— *Chandra* 0.3 – 7 keV (color) and VLA 1.4 GHz (contours) images of GB 1428+4217 showing the bright core and faint $\sim 3.6''$ distant jet knot at $PA \sim 295^\circ$. Coordinates are in J2000.0 equinox. The X-ray data are binned by 1/2 of the native $0.492''$ pixels and Gaussian smoothed with kernel radius of 3 pixels. The 10 radio contours start at 0.17 mJy/bm (4 times the off-source rms) increasing by factors of 2 up to 87 mJy/bm (peak is 155.4 mJy/bm) with circular beamsize = $1.5''$.

tions of GB 1428+4217 on 2004 Dec 6 (program AC755) at 1.4 and 4.9 GHz. Data were recorded in two 50 MHz wide channels centered at 1.385 and 1.465 GHz, and 4.835 and 4.885 GHz, respectively. In the 1.4 GHz image (2020 s exposure; off-source rms noise = 0.043 mJy/bm) shown in Figure 1, we discovered a $3.6''$ distant jet knot at a position angle (PA) of -66° with a flux density of 1.4 mJy (10% uncertainties are assumed in the radio measurements for the knot). Because no counterpart was detected in the shallower 4.9 GHz image (710 s), we obtained deeper (1 hr exposure; rms = 0.022 mJy/bm) follow-up B-array observations at this frequency on 2008 Jan 13 (program S8723) matching the resolution of the A-array 1.4 GHz discovery data. The knot is confirmed at 4.9 GHz with a flux density of 0.41 mJy and the resultant 1.4 – 4.9 GHz radio spectral index is $\alpha_r = 1.0 \pm 0.1$. Model-fitting the radio nucleus and knot in the 1.4 GHz (u, v) data using DIFMAP (Shepherd et al. 1994), we found that both features are unresolved at $\sim 1''$ resolution and set this as the upper limit to the size of the knot.

Our *Chandra* observation of GB 1428+4217 was obtained on 2007 Mar 26 (obsid 7874) as part of a small snapshot program targeting four $z > 3.6$ flat-spectrum radio quasars with detected radio jets in the aforementioned VLA survey (Cheung et al. 2005). Of these four targets, the X-ray jet detections of GB 1428+4217 and one other target (PKS 1418–064 at $z = 3.7$), were initially reported in Cheung et al. (2008). The full results of the survey will be reported elsewhere together with the *Chandra*/VLA results for an additional seven $z = 2 - 3$ quasars with radio jets obtained as part of other programs.

In the 11.7 ks *Chandra* observation of GB 1428+4217, we used the nominal aim-point of the ACIS-S3 chip and a 1/8th sub-array mode (0.4 s frame time) in order to mitigate pileup of the nucleus. We reprocessed the data by

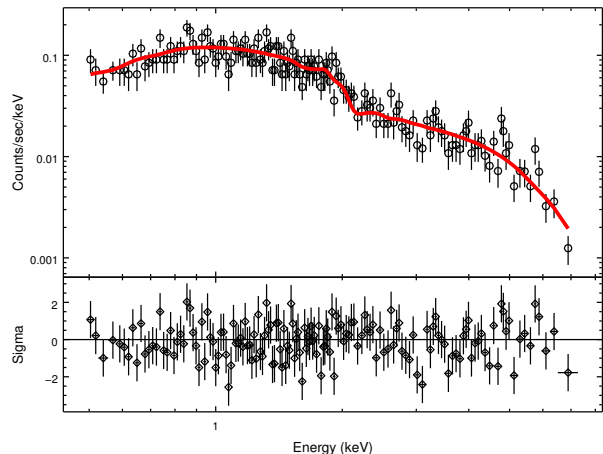


FIG. 2.— *Chandra* ACIS-S 0.5 – 7 keV spectrum of the quasar nucleus in the (top) panel. The absorbed power-law model overlaid in red, and the deviations from the model in the (bottom) panel. The data were grouped in bins with a minimum of 10 counts per bin.

using `chandra_repro` script in CIAO 4.4 (Fruscione et al. 2006) and assigned the most recent instrument calibration available in CALDB 4.5. The script also runs `acis_process_events` which applies the sub-pixel algorithm and provides the data with the best angular resolution required by our analysis. With the correction for 9.4% deadtime, we have 10.6 ks effective exposure time on the source. The astrometry was set by adjusting the X-ray core position to that of the VLBI radio position from Fey et al. (2004), R.A. = $14^{\text{h}}30^{\text{m}}23^{\text{s}}.742$, Decl. = $+42^{\circ}04'36.49''$ (J2000.0).

More than 2200 counts were detected from the quasar X-ray core, allowing for spectral analysis. Model fitting of the quasar data was performed with a $1.5''$ radius circular aperture. A pie region excluding the jet was used to determine the background. The spectrum was well fit with an absorbed power law model (Figure 2), with fixed Galactic absorption, N_{H} . The *Chandra* derived parameters are consistent with the *XMM* results published by Worsley et al. (2006), with the power-law spectral index slightly smaller in our *Chandra* spectrum, which may be due in part to pileup. Applying the `jdpileup` model (Davis 2001), the core is only 2.7% piled up and the resulting parameters are essentially unchanged, but the statistical uncertainties increased (see Table 1).

X-ray emission coincident with the $3.6''$ distant radio jet knot is apparent in the smoothed *Chandra*-ACIS image (Figure 1). The charge transfer readout streak is at $PA = 43^\circ$, i.e., almost perpendicular to the jet axis, so does not contaminate the knot’s emission. For the knot, we defined an elliptical aperture region giving 20.3 ± 4.8 net counts in the 0.3 – 7 keV range. The spectrum of this emission extends up to a rest frame energy of $\sim 6.5 (1+z)$ keV = 37 keV, and is quite soft with 14.9 net counts between 0.5 – 2 keV and only 4.4 between 2 – 7 keV. The fluxes resulting from a spectral fit assuming a single power law with $\alpha_x = 0.7$ frozen and Galactic N_{H} are presented in Table 1. For the given flux of the jet, its isotropic luminosity as measured in the observer rest frame in the 0.5–10 keV band would be 4.0×10^{45} erg s $^{-1}$.

TABLE 1
 GB 1428+4217 X-RAY SPECTRAL FITS

Component Model (1)	α_x (2)	$N_H(z=4.72)$ (3)	$F(0.5-2 \text{ keV})$ (4)	$F(2-10 \text{ keV})$ (5)
Core Power-Law	$0.38^{+0.09}_{-0.06}$	< 3.6	5.5 ± 0.5	$16.4^{+3.3}_{-2.7}$
Core Power-Law with pileup	$0.43^{+0.25}_{-0.12}$	< 4.9	6.1 ± 0.7	$16.7^{+5.8}_{-4.4}$
Jet Power-Law	0.7 (fixed)	–	$5.7^{+1.8}_{-2.2} \times 10^{-2}$	$10.8^{+4.2}_{-3.3} \times 10^{-2}$

(1) Component and source model. All fits assume Galactic $N_H = 1.4 \times 10^{20} \text{ cm}^{-2}$ fixed (Dickey & Lockman 1990). Uncertainties are 90% for one significant parameter and upper limits are quoted at 3σ .

(2) We use the definition of spectral index, α , as $F_\nu \propto \nu^{-\alpha}$.

(3) Intrinsic absorption at $z=4.72$ in units of 10^{22} cm^{-2} .

(4, 5) Unabsorbed flux in the observed energy range in units of $10^{-13} \text{ erg s}^{-1} \text{ cm}^{-2}$. The absorbed $F(0.5-2 \text{ keV})$ values are 14 – 15% smaller assuming that the absorber has the N_H value set at the 3σ limit.

To help constrain the overall spectral energy distribution (SED) of the $3.6''$ knot, we analyzed an archival *HST* WFPC2 image from 1999 Feb 8 (total exposure: 9.4 ks) with the F814W filter (program 7266). Within a circular aperture ($r = 0.5''$) centered on the knot, we found no significant excess optical emission with respect to the background measured from six adjacent regions. From the aperture count rates, we derive an aperture corrected (Holtzman et al. 1995) upper limit of $< 0.13 \mu\text{Jy}$ (3σ) at $3.74 \times 10^{14} \text{ Hz}$ from the knot.

Finally, to search for radio jet emission on smaller scales, we analyzed VLBI 2.3 and 8.6 GHz data for GB 1428+4217 obtained in 1998 Feb 10 as part of the USNO RRFID⁹ project (Fey et al. 2004). The calibrated (u, v) data were reimaged and self-calibrated, revealing a one-sided jet extending west of the core (Figure 3). The jet is visible in the 2.3 GHz map out to 30 mas ($\sim 200 \text{ pc}$, projected). This jet can be modeled as three knots at $PA = -96^\circ$ to -117° with a total flux density of 9.5 mJy. Utilizing the closest (and brightest) jet knot, we measure a jet to counterjet flux ratio defined as the peak / ($3 \times$ rms noise) = $3.3 \text{ mJy} / 3 \times 0.16 \text{ mJy} \approx 7$. Most of the pc-scale jet is resolved out in the higher resolution 8.6 GHz image, where the jet extends out to only 3 mas (2.4 mJy). On smaller scale, Veres et al. (2010) found a faint $\sim 1 \text{ mas}$ extension in VLBA 15 GHz data also in the same direction. The pc-scale jet deviates by about 30° from the large-scale *Chandra*/VLA knot; however, its existence makes the jet interpretation for the kpc-scale emission more likely.

3. DISCUSSION

The kpc-scale radio and X-ray jet reported here in the $z = 4.72$ blazar GB 1428+4217 is the highest-redshift example thus far. Together with the blazar nature of its core emission (Section 1), the one sidedness of the kpc-scale and $\sim 200 \text{ pc}$ scale jet seen in our VLBI images imply that the jet is relativistic and probably aligned at a small angle, θ , to our line of sight. For $\theta \lesssim 20^\circ$, the $3.6''$ knot distance from the core corresponds to $24/(\sin \theta) \text{ kpc} \gtrsim 70 \text{ kpc}$, deprojected for the detected jet. This is far enough from its parent host galaxy that the most significant source of seed photons for inverse Compton scattering is the cosmic microwave background (CMB). This is especially relevant at $z=4.72$, where the CMB en-

ergy density for an observer at rest at the source redshift is $u_{\text{CMB}}^* = 4.2 \times 10^{-13} (1+z)^4 = 4.5 \times 10^{-10} \text{ erg cm}^{-3}$, i.e., 1070 times greater than it is locally.

The radio and X-ray morphology of GB 1428+4217 at $z = 4.72$ is nearly identical to that of the $z = 4.3$ quasar GB 1508+5714 with similar X-ray (Siemiginowska et al. 2003; Yuan et al. 2003) and radio (Cheung 2004; Cheung et al. 2005) luminosities in the jet. Both show single radio features separated from the bright nucleus and display steep spectra (with spectral indices, $\alpha_r = 1.0 \pm 0.1$ and 1.4 ± 0.2 , respectively). Because of poor statistics, the X-ray spectrum in GB 1428+4217 is unconstrained and can not be compared with that of GB 1508+5714 where $\alpha_x \approx 0.9 \pm 0.4$ was determined. In GB 1428+4217, we calculate the ratio $f_x/f_r \equiv (\nu_x F_x) / (\nu_r F_r) = 205$, using monochromatic flux densities at 1 keV and 1.4 GHz. This is larger than the $z = 4.3$ case where $f_x/f_r = 158$, and larger than found in other lower- z examples (cf., Cheung 2004; Massaro et al. 2011). Equivalently, $f_x/f_r = 205$ corresponds to a radio to X-ray spectral index, $\alpha_{rx} = 0.72$. Although α_{rx} is just consistent with the limit on the radio to optical spectral index, $\alpha_{ro} > 0.73$, it is smaller than the radio spectral index, $\alpha_r = 1.0$, indicating that the X-rays are not a simple extension of the radio synchrotron spectrum.

The X-ray emission could correspond to either inverse Compton emission of the low-energy electrons involving CMB target photon field (‘IC/CMB’ model; Tavecchio et al. 2000; Celotti et al. 2001), or an additional synchrotron component due to a higher-energy electron population (e.g., Stawarz et al. 2004; Hardcastle 2006). Overall, the broad-band spectral indices appear consistent with the $(1+z)^4$ amplification of the CMB energy density, $f_x/f_r \sim (\delta/\Gamma)^2 u'_{\text{CMB}}/u'_B \propto (1+z)^4 (\delta/B)^2$ (with the Doppler factor, δ , the bulk Lorentz factor, Γ , and the CMB and magnetic field energy densities in the jet rest frame, $u'_{\text{CMB}} = \Gamma^2 u_{\text{CMB}}^*$ and $u'_B = B^2/8\pi$, respectively), as would be expected in the IC/CMB model (e.g., Schwartz 2002; Cheung 2004). Following Cheung (2004), we apply the IC/CMB model assuming also equipartition with a relativistic electron spectrum with power-law slope, $p = 2\alpha + 1 = 3$, extending down to a minimum $\gamma = 10$, in a sphere with an apparent size of $1.8 \times 1''$ for the GB 1428+4217 jet knot (see Marscher 1983). For the case where the jet Lorentz factor is set equal to the Doppler factor, we derive $\Gamma = \delta = 4.7$, and

⁹ This research has made use of the United States Naval Observatory (USNO) Radio Reference Frame Image Database (RRFID).

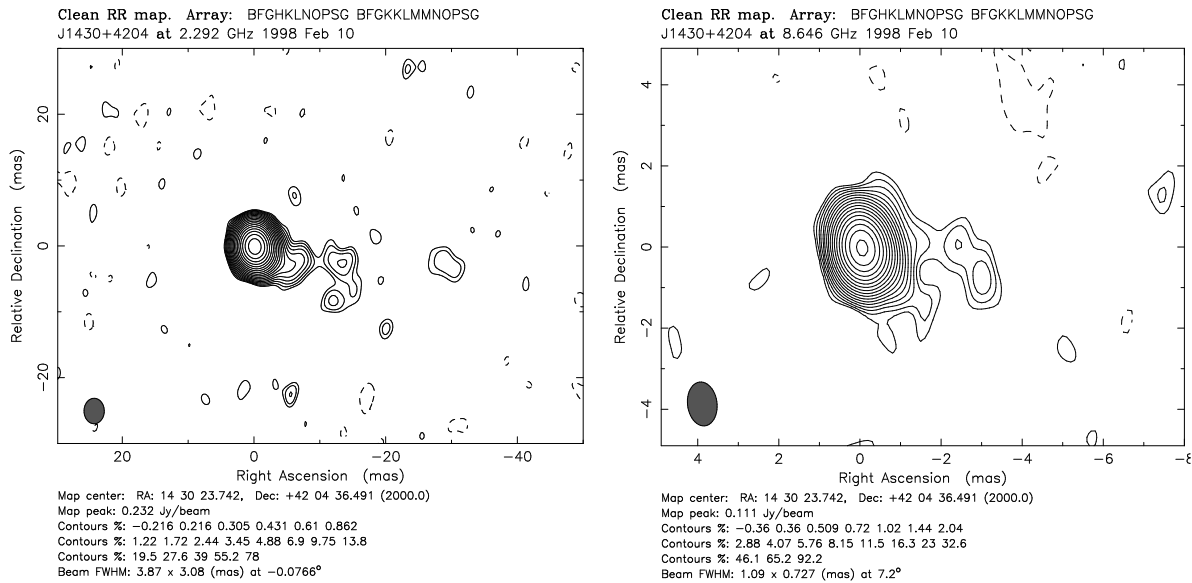


FIG. 3.— VLBI 2.3 GHz (left) and 8.6 GHz (right) images of GB 1428+4204 from reprocessing USNO data (Fey et al. 2004). Note the difference in scales. The contours begin at 0.5 (3.87 mas \times 3.08 mas) and 0.4 mJy/bm (1.09 mas \times 0.73 mas), respectively, and increase by factors of $\sqrt{2}$. The bright core with the one-sided pc-scale jet to the west is apparent.

a magnetic field in the jet rest frame, $B = 35 \mu\text{G}$. These parameters are fairly insensitive to the extrapolation of the $p = 3$ slope down to low energies and our conservative upper limit to the radio knot size. Assuming instead a typical observed radio jet spectral index of 0.75 at lower-redshifts (following Kataoka & Stawarz 2005), and the knot diameter is $0.6\times$ smaller than the assumed $1''$ limit, we obtain $B = 21 \mu\text{G}$ and $\delta = 6.3$. These estimates assume a single X-ray/radio emitting zone applies to our $\sim 1''$ (6.6 kpc) angular resolution element.

Similarly applying the IC/CMB model to the other high-redshift X-ray jet, GB 1508+4714 ($z = 4.3$; Cheung 2004) and 1745+624 ($z = 3.9$; Cheung et al. 2006), they derived $\delta \sim 3 - 5$. These values are smaller than the typical ones ($\delta \sim 5 - 10$) determined for lower-redshift jets (e.g., Kataoka & Stawarz 2005). Although the number of quasar X-ray jets found at such very high-redshifts ($z \sim 4-5$) is still small, the slower large-scale jets implied in our analysis for the current sample seem to indicate that they are either: (1) intrinsically less relativistic, or (2) decelerate more rapidly out to $\sim 10^3 - 10^4$ kpc-scales than their lower-redshift counterparts. In the first case, this would be consistent with the recent finding that the relative abundance of high-power blazars relative to the parent population of radio-loud quasars and radio galaxies decreased substantially above $z \sim 3$, likely as a result of a decrease of the average bulk Lorentz factor of blazar jets in the early Universe (see Volonteri et al. 2011). The latter possibility could be supported by the fact that the environments of high-redshift ($z > 2$) radio sources are believed to reside in more inhomogeneous and multi-phase environments than in nearby radio sources (see e.g., Rees 1989; De Young 2006), and this may manifest in the slower large-scale jets due to an enhanced entrainment of the ambient gas when the jet propagates through the host galaxy.

An argument put forth against the IC/CMB model comes from observations of the unresolved (at *Chandra*

resolution) quasar “cores” at high-redshift. In this interpretation for the kpc-scale emission, one may expect that the X-ray emission in these cores could also be enhanced, as they contain an unresolved portion of the jet (which we know are highly relativistic from, e.g., VLBI superluminal motion studies). This could manifest in different X-ray core properties at high- z (X-ray, and optical-to-X-ray spectra), but *Chandra* studies thus far show no such trends with redshift (e.g., Lopez et al. 2006). However, these analyses are hampered by the fact that most of the sources analyzed so far in this context are only moderately radio-loud, and in general, only a small fraction of jets in radio-loud quasars extend to kpc-scales (e.g., Bridle & Perley 1984; Liu & Zhang 2002).

The radio structures of higher-redshift samples are now being investigated in more detail (Gobeille 2011, Gobeille et al., in preparation), and will pave the way for further *Chandra* X-ray studies. X-ray observations of a larger sample of kpc-scale radio jets over a broad redshift range ($z > 2$) should provide further elucidation of the correct X-ray emission mechanism which will give us insight on the deeper physics contained in the data. Such high redshift systems allow us to study jets which result from the “earliest” actively accreting black hole systems. As most detections are currently at $z \lesssim 2$, we have begun to study more distant examples and these results will be presented in a future paper.

Acknowledgments

This research was supported in part by NASA through contract NAS8-39073 (A. S., D. E. H., D. A. S.) and *Chandra* Award number GO7-8114 issued to NRAO and Eureka Scientific (C. C. C.) and Brandeis University (D. G., J. F. C. W.) by the *Chandra* X-Ray Observatory Center, which is operated by the Smithsonian Astrophysical Observatory for and on behalf of NASA under contract NAS8-39073. Radio astronomy at Brandeis

University is supported by NSF grant NSF1009261. This work began while C. C. C. was supported by a Jansky fellowship from NRAO; his work at NRL is supported in

part by NASA DPR S-15633-Y.

Facilities: CXO (), VLA (), HST (WFPC2)

REFERENCES

- Bridle, A. H., & Perley, R. A. 1984, *ARA&A*, 22, 319
 Celotti, A., Ghisellini, G., Chiaberge, M. 2001, *MNRAS*, 321, L1
 Cheung, C. C. 2004, *ApJ*, 600, L23
 Cheung, C. C., Wardle, J. F. C., Lee, N. P. 2005, in 22nd Texas Symposium on Relativistic Astrophysics, Eds. P. Chen et al. (Palo Alto: SLAC), 1613
 Cheung, C. C., Stawarz, L., Siemiginowska, A. 2006, *ApJ*, 650, 679
 Cheung, C. C., et al. 2008, in "Extragalactic Jets: Theory and Observation from Radio to Gamma Ray," Eds. T. A. Rector & D. S. De Young, ASP Conf. Ser. 386, 462
 Davis, J. E. 2001, *ApJ*, 562, 575
 De Young, D. 2006, *Astron. Nachr.*, 327, 231
 Dickey, J. M., & Lockman, F. J. 1990, *ARA&A*, 28, 215
 Fabian, A. C., Brandt, W. N., McMahon, R. G., Hook, I. M. 1997, *MNRAS*, 291, L5
 Fabian, A. C., et al. 1999, *MNRAS*, 308, L6
 Fey, A. L., et al. 2004, *AJ*, 127, 3587
 Fruscione, A., et al. 2006, *Proc. SPIE*, 6270, 60
 Gobeille, D. 2011, PhD thesis, Brandeis University
 Hardcastle, M. J. 2006, *MNRAS*, 366, 1465
 Harris, D.E., & Krawczynski, H. 2006, *ARA&A*, 44, 463
 Holtzman, J. A., et al. 1995, *PASP*, 107, 1065
 Hook, I. M., & McMahon, R. G. 1998, *MNRAS*, 294, L7
 Kataoka, J., & Stawarz, L. 2005, *ApJ*, 622, 797
 Liu, F. K., & Zhang, Y. H. 2002, *A&A*, 381, 757
 Lopez, L. A., et al. 2006, *AJ*, 131, 1914
 Marscher, A. P. 1983, *ApJ*, 264, 296
 Massaro, F., Harris, D. E., Cheung, C. C. 2011, *ApJS*, 197, 24
 Miley, G., & De Breuck, C. 2008, *A&A Rev.*, 15, 67
 Rees, M. J. 1989, *MNRAS*, 239, 1P
 Schwartz, D. A. 2002, *ApJ*, 569, L23
 Shepherd, M. C., Pearson, T. J., Taylor, G. B. 1994, *BAAS*, 26, 987
 Siemiginowska, A., et al. 2003, *ApJ*, 598, L15
 Stawarz, L., Sikora, M., Ostrowski, M., & Begelman, M. C. 2004, *ApJ*, 608, 95
 Tavecchio, F., Maraschi, L., Sambruna, R. M., Urry, C. M. 2000, *ApJ*, 544, L23
 Veres, P., Frey, S., Paragi, Z., Gurvits, L. I. 2010, *A&A*, 521, A6
 Volonteri, M., Haardt, F., Ghisellini, G., & Della Ceca, R. 2011, *MNRAS*, 416, 216
 Worsley, M. A., Fabian, A. C., Pooley, G. G., Chandler, C. J. 2006, *MNRAS*, 368, 844
 Yuan, W., Fabian, A. C., Celotti, A., Jonker, P. G. 2003, *MNRAS*, 346, L7